Decision-support Measure for Resilient Infrastructure Networks Considering Operation Mechanism and Cascading Failure

Y. Kwon
Graduate Student, Dept. of Civil and Environmental Engineering, Seoul National University, Seoul, South Korea

J. Song
Professor, Dept. of Civil and Environmental Engineering, Seoul National University, Seoul, South Korea

ABSTRACT: While the scale and frequency of disasters increase worldwide, infrastructure networks have become more complex as urbanization progresses. In efforts to maintain the network's performance through an appropriate decision-making process, disaster resilience is considered an essential ability of the systems. Recently, a system-reliability-based disaster resilience analysis framework was proposed to fully consider the relationship between the states of the system and the components. The proposed framework hinges on the reliability-redundancy (β-π) analysis, which enables a decision-maker to identify disruption scenarios critical to the system-level resilience. Based on the β-π analysis method, this study aims to overcome limitations of existing component reliability importance measures in terms of adaptability to the target resilience of the system, considering the sequential component failures due to network flow redistributions, and excluding the spurious correlation caused by common source effects of the disastrous events. The proposed measure considers the effects of cascading failures by merging the causal effect of the state transition of the component in the disruption scenario on the change in the system state. Given the probabilistic information of the lines, electrical properties, and topology of the power grid, the proposed measure is computed to further support decision-making processes.

1. INTRODUCTION

As a response to the increasing socio-economic demands, modern society is increasing the size and complexity of major infrastructure networks such as power grids, water and sewage systems, and transportation networks. Under these circumstances, accelerating climate change further exacerbates the safety and vulnerability of the system. Accordingly, the concept of *Disaster Resilience*, which is defined as the holistic ability of an infrastructure to cope with external risks, is being developed (Bruneau et al., 2003). Depending on the scale and type of civil infrastructure, the system-level performance and the states of components in the system are defined differently, so it is necessary to approach the disaster resilience of the systems separately. To manage the disaster resilience of infrastructure, decision-making processes are usually carried out component-wise. In addition, appropriate disaster resilience assessment should aim to provide a basis for decision-making to secure the target resilience by incorporating the relationship between the states of components and the system, and the uncertainty in the state of the components (Lim et al., 2022).

For these reasons, it is crucial to prioritize individual components by identifying their impact on the system-level performance. Various component importance measures (CIMs) have been developed to quantify the contribution of a component to system performance as useful decision-supporting measures (Der Kiureghian, 2022). However, the existing IMs are defined with simple mathematical expressions based on the correlation between the states of components, which can consider nonrelevant components as important ones from a system reliability perspective.

Among various types of infrastructure networks, this paper focuses on a power grid, a system in which the state of components is determined by the power flows between them. This paper aims to demonstrate the effectiveness of the recently proposed system-reliability-based disaster resilience analysis framework (Lim et al., 2022) at the infrastructure network scale through its applications to the power grid. In addition, a new decision-support measure based on the framework is proposed to consider the operation mechanism of the system and the cascading failures. The measure incorporates the causal influence of the external hazards on the component state and that of the component state on the final system state. Finally, the paper concludes with discussions of the disaster resilience analysis of the power grid and the applicability of the proposed measure.

2. BACKGROUND KNOWLEDGE

2.1. System-reliability-based disaster resilience analysis framework (S-DRA)

Lim et al. (2022) characterized the disaster resilience of a civil infrastructure system by three criteria at three scales of the system, which led to a '3x3 resilience matrix.' Table 1 shows a part of the matrix for the infrastructure network scale. Infrastructure networks are usually described with nodes and interconnecting links. Since these node- and link-type components are distributed over a large area, *Reliability* should be evaluated with appropriate consideration of the spatial correlation between the component states and variability. To evaluate *Redundancy* of the system, the eventual system-level degradation due to sequential failures triggered by initial component disruption should be considered.

Table 1: Three resilience criteria of infrastructure network scale in the '3x3 resilience' matrix.

Criteria \ *Scale*	*Infrastructure network*
Reliability	*Avoiding initial disruption of network components*
Redundancy	*Preventing cascading failures causing degradation of network performance*
Recoverability	*Executing proper actions for loss of network functionality*

The S-DRA framework evaluates the *reliability* and *redundancy* criteria in the generalized indices form. For the *i*th initial disruption scenario F_i, the reliability index β_i and redundancy index π_i are defined as

$$\beta_i = -\Phi^{-1}\big(P(F_i|H)\big) \tag{1}$$

$$\pi_i = -\Phi^{-1}\left(P\big(F_{sys}\big|F_i, H\big)\right) \tag{2}$$

where $\Phi^{-1}(\cdot)$ stands for the inverse of the standard normal cumulative distribution function (CDF), and H and F_{sys} denote external hazard and system-level failure, respectively.

The framework sets the probability of final system-level failure as the standard of the disaster resilience level. The system failure probability caused by F_i can be computed using the conditional probabilities in Eqs. (1) and (2), and should be managed below the "*de minimis* risk," the threshold probability of the risks that society can or decides to neglect, i.e.,

$$P\big(F_{sys,i}\big) = P\big(F_{sys}\big|F_i, H\big)P(F_i|H)\lambda_H < P_{dm} \tag{3}$$

where λ_H denotes the mean occurrence rate of H. P_{dm} is set as $10^{-7}/year$ (Paté-Cornell, 1994) in this paper. Dividing Eq. (3) by λ_H, disaster resilience constraint $\mathcal{D}_H$ can be expressed as

$$\mathcal{D}_{\lambda_H}: \Phi(-\pi_i)\Phi(-\beta_i) < \frac{P_{dm}}{\lambda_H} \tag{4}$$

The scatter plot of the pair of redundancy and reliability indices, (π, β), along with the disaster resilience constraint in Eq. (4) is called the β-π diagram. This graphical representation helps identify critical disruption scenarios and guide proper decision-making strategies at both component- and system-level viewpoints.

2.2. Power flows by operation mechanism and cascading failures

In a power grid, the power is distributed on the lines according to the electrical properties of lines and Kirchhoff laws. In this paper, direct current (DC) power flow is applied to consider only the flow of active power (Grainger, 1999).

DC power from bus i to bus j is formulated as

$$f_{ij} = \frac{1}{x_{ij}}(\theta_i - \theta_j) = b_{ij}(\theta_i - \theta_j) \qquad (5)$$

where θ_i and θ_j are the voltage phase of bus i and j, respectively, and x_{ij} and b_{ij} are the reactance and the susceptance of the line l_{ij} connecting two buses, respectively. The active power flow of bus i is a sum of the flows of all l_{ij}'s in Eq. (5), i.e.,

$$P_i = \sum_j f_{ij} = \sum_j b_{ij}(\theta_i - \theta_j) \qquad (6)$$

In a matrix form, Eq. (6) is rewritten as

$$\mathbf{P} = \mathbf{B\Theta} \qquad (7)$$

where $\mathbf{P}$ is the vector of real power injections, $\mathbf{\Theta}$ is the vector of voltage angles, and $\mathbf{B}$ is the susceptance matrix for all buses. The diagonal element of $\mathbf{B}$ is the sum of the line susceptance connected to bus i, and the off-diagonal term of $\mathbf{B}$ is the minus of the line susceptance, i.e., $B_{i,i} = \sum_i b_{ij}$, and $B_{i,j} = -b_{ij}$. The power flow in l_{ij} is obtained by substituting the voltage angle vector $\mathbf{\Theta} = \mathbf{B}^{-1}\mathbf{P}$ in Eq. (7) to Eq. (5).

The power grids will operate normally according to Eqs. (5)-(7) if there are no threats. However, if some lines are disrupted by external threats, power flows are redistributed to create additional loads on other lines. Since the power grids are operated to protect the individual line, the lines with an assigned flow greater than their capacity (overloaded) are automatically turned off before they break down. Continuous line shutdowns by the growing overloads are referred to as cascading failures in power grids.

The cascading failures may cause huge degradation in the system performance, e.g., a blackout in power grids. Here, a model to simulate the cascading failures can provide guides to evaluate the disaster resilience of the eventual system by analyzing which lines will be threatened in the next cascading stage (nearby or sudden far lines) in advance.

2.3. Do-operators in causal diagrams

A causal diagram is a directed acyclic graph (DAG) describing the causal relationship between random variables of interest. It consists of nodes representing random variables and arrows indicating the causal influence between the variables. The well-constructed causal diagram facilitates answering causal queries, e.g., how much certain component disruption will affect the system performance, using only the observed data without further experiments.

Let us consider a causal diagram in Figure 1 with binary variables, S, W, X, Y, and Z. For the causality-based query, "How much does X affect Y?", the conditional probability $P(Y = y|X = x)$ does not provide the answer since it gives varying values as the state of X changes, i.e., $P(Y = y|X = x) \neq P(Y = y|X \neq x)$, even though there is no direct causality from X to Y.

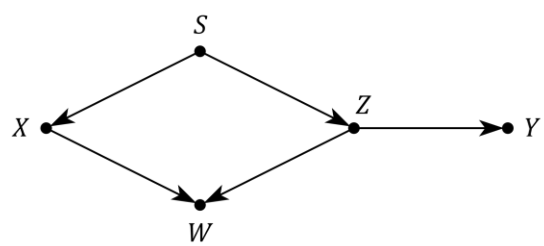

Figure 1: Causal diagram of five binary variables.

The common source S fundamentally makes it impossible to answer the query about the causality between X and Y with observable data. To give the right answer excluding spurious associations, the probability with a *do*-operator, denoted $do(\cdot)$, is proposed as

$$P\big(Y = y \big| do(X = x)\big) \qquad (8)$$

which fixes X at an outcome x and deletes all arrows heading into X in the causal diagram before probabilistic inferences (Pearl, 2009). Since the *do*-operator represents the intervention of the "what if" condition, it can quantify the causal effect by the change in the probability caused by the opposite outcome, $X \neq x$. The difference or the ratio is often adopted depending on the analysis purpose (Pearl, 2001).

Back-door criterion is one of the well-known methods to compute the term with the *do*-operator. A variable set A for a pair (X, Y) in a causal diagram is referred to as a sufficient set that meets the back-door criterion if they satisfy two conditions: (1) No elements in A are descendants of X, and (2) A blocks every path between X and Y that contains an arrow into X. Then, Eq. (8) can be computed by

$$\sum_a P(Y = y | X = x, A = a) P(A = a) \tag{9}$$

where a denotes all outcomes of A. Since a set $\{Z\}$ meets the back-door criterion for (X, Y) in Figure 1, the probability with *do*-operator in Eq. (8) can be computed as Eq. (9), i.e.,

$$\begin{aligned} &P(Y = y | X = x, Z = z) P(Z = z) \\ &\quad + P(Y = y | X = x, Z \neq z) P(Z \neq z) \\ &= P(Y = y | Z = z) P(Z = z) \\ &\quad + P(Y = y | Z \neq z) P(Z \neq z) \end{aligned} \tag{10}$$

which is consistent regardless of the state of X.

2.4. Component importance measures (CIMs)

CIMs quantify the relative contribution of a certain component to the system's performance. Table 2 summarizes the definitions of four CIMs (Der Kiureghian, 2022): risk achievement worth (RAW), risk reduction worth (RRW), Fussell-Vesely (FV), and conditional probability (CP). E_e is a failure event of component e, C_l is the lth min-cut set of the system, $\mathcal{C}_l$ is the failure event of components in C_l, and F_{sys+e} and F_{sys-e} is a system failure event when component e is guaranteed to fail and survive, respectively.

Table 2: Mathematical definitions of component importance measures: RAW, RRW, FV, and CP.

RAW_e	$P(F_{sys+e})/P(F_{sys})$
RRW_e	$P(F_{sys})/P(F_{sys-e})$
FV_e	$P(\bigcup_{l:e \subseteq C_l} \mathcal{C}_l)/P(F_{sys})$
CP_e	$P(F_{sys} \| E_e)$

3. APPLICATION OF S-DRA TO THE POWER GRID

Figure 2 shows a power grid consisting of 14 buses and 20 branches. The power grid is a system in which the locations of the buses are determined based on the IEEE 14 Bus Test Case. Only the branches are considered the components of interest. Under a potential earthquake scenario with a magnitude of 7.5, the S-DRA framework is applied to the power grid.

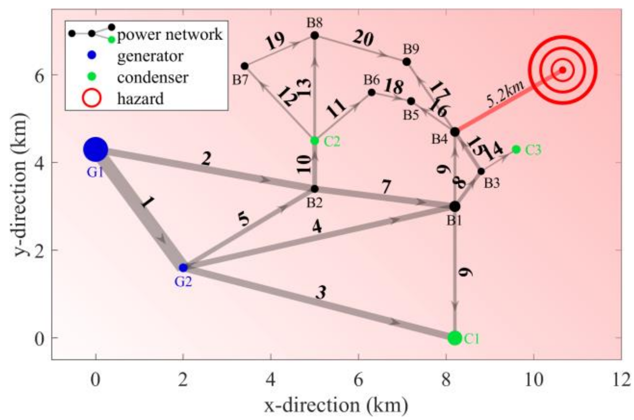

Figure 2: Power grid from IEEE 14 Bus Test Case with an earthquake scenario.

The demand intensity is set as a peak ground acceleration (PGA) acting in the middle of the component by the seismic hazard. The general ground-motion prediction equation (GMPE) on component i is formulated as

$$\ln D_i = F(M, R_i) + \eta + \varepsilon_i \tag{11}$$

where D_i is PGA at component i, $F(\cdot)$ is a ground-motion model (GMM) with input variables M and R_i, M is the magnitude of the earthquake, R_i is the distance between the epicenter and component i, and η and ε_i are inter- and intra-event residuals, respectively.

3.1. Reliability index

Reliabilities of the components are obtained by the fragility analysis against the earthquake. The component state is expressed by combinations of applied PGA and the seismic capacities of the components. Assuming that the seismic capacity of the components follows a lognormal distribution, the reliability index for a certain damage state (DS) is derived from Eq. (11) as

$$\beta_i = -\Phi^{-1}\big(P(E_i|H)\big) = \frac{\ln \alpha_{DS}^i - F(M, R_i)}{\sqrt{\left(\beta_{DS}^i\right)^2 + \sigma_T^2}} \quad (12)$$

where σ_T^2 is the total variance of GMPE, a sum of the variances of two residuals, and α_{DS}^i and β_{DS}^i are the lognormal fragility parameters, i.e., the median and the standard deviation of the capacity of component i.

The GMPE and the variances of two residuals are adopted from Boore and Atkinson (2008) in this paper. The fragility parameters α_{DS} and β_{DS} are assumed as 2.0 and 1.1, respectively for the components over 3km in length, and 0.7 and 0.8, for the components less than 3km in length. Figure 3 shows the failure probability of twenty components calculated using the reliability index in Eq. (12).

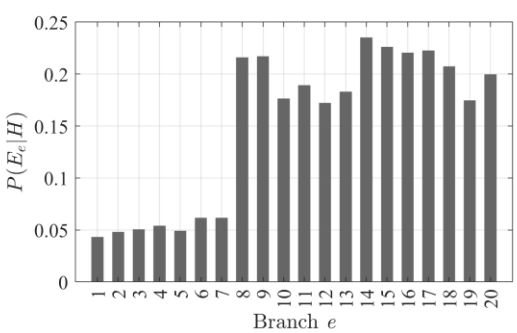

Figure 3: Probability of branch failures.

For component i, a safety factor Z_i of $P(E_i|H) = P(Z_i < -\beta_i)$ is assumed to follow the multivariate normal distribution. The correlation coefficient between the safety factors for different components i and j separated by distance Δ (km) is expressed as

$$\rho_{ij} = \frac{\sigma_\eta^2 + \rho_{\varepsilon_m \varepsilon_n}(\Delta)\sigma_\varepsilon^2}{\sqrt{\left\{\left(\beta_{DS}^i\right)^2 + \sigma_T^2\right\}\left\{\left(\beta_{DS}^j\right)^2 + \sigma_T^2\right\}}} \quad (13)$$

where $\rho_{\varepsilon_i \varepsilon_j}(\Delta)$ is the spatial correlation model (Lee and Song, 2022). The spatial correlation is set as $\exp(-0.27\Delta^{0.40})$ in this paper.

3.2. Redundancy index

To evaluate the final system state initiated by the disruption scenario, the intermediate cascading failure needs to be analyzed. The electrical power capacity of all components is set to a tolerance multiplication of the initial power flow for the intact system (tolerance is set as 1.5 in this paper). In every stage of the cascading failure, components with the reassigned flow exceeding the capacity are considered overloaded and turned off in the next stage. If no components are overloaded anymore, the system is considered in the final state.

Figure 4 shows the power capacity of the components. In the final state of the system, components connected to the generations are considered to survive. The system-level performance is set as the ratio of the sum of the capacity of the operating components in the final system to that in the intact system. System failure occurs when system-level performance is below a certain threshold, 0.3 in this paper.

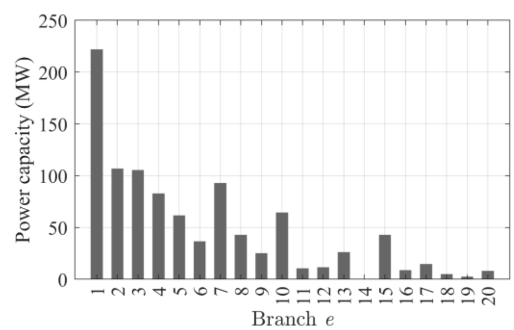

Figure 4: Power capacity of branches.

3.3. β-π diagram

To investigate the effect of multiple component failures, F_i^k is defined as the ith initial disruption scenario involving failures of k components in a set I_i^k. The resilience indices pair $R_i^k = \left(\pi_i^k, \beta_i^k\right)$ becomes $\left(-\Phi^{-1}\left(P\left(F_{sys}\middle|F_i^k\right)\right), -\Phi^{-1}\left(P\left(F_i^k\middle|H\right)\right)\right)$ similarly to Eqs. (1) and (2). To compute the resilience pairs for k (≥ 2), reliabilities in Eqs.

(12) and correlation coefficients in Eq. (13) are substituted to multivariate normal CDF.

Figure 5 shows the β-π diagram of the power grid according to the number of initial disruptions, k. The β-π diagram facilitates identifying critical scenarios that lead to socially unacceptable risk. For example, when $\lambda_H = 10^{-5}\,year$, among twenty initial disruption scenarios for $k = 1$, only components *5*, *6*, and *7* satisfy D_{λ_H} in Eq. (4).

It is observed that the markers tend to spread to the upper left direction as k increases, i.e., resulting in a higher reliability index and lower redundancy index. This is because the likelihoods of scenarios involving more component failures are relatively low, but once such disruption occurs, the network's capability to avoid system-level failures drops significantly. In addition, the reliability indices are distributed in clusters. It is attributed to the consistent and lower failure probabilities of components *1* to *7* than the rest of the components in Figure 3.

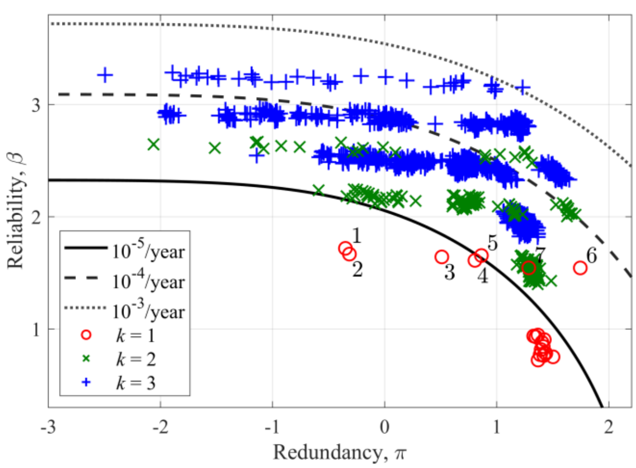

Figure 5:β-π diagram of the power grid.

4. NEW DECISION-SUPPORT MEASURES FOR POWER GRIDS

Based on the results of the β-π analysis, a new decision-support measure is proposed for the power grids reflecting the causal influences of the cascading failures.

4.1. Proposal of causality-based measures

Figure 6 is the proposed causal diagram, showing the causal relationships between unobservable variable U, hazard source S_j $(j = 1, 2, \cdots, m)$, component state X_e $(e = 1, 2, \cdots, n)$, the final component state after the cascading failures, C_i $(e = 1, 2, \cdots, n)$, and the final system state Y_{net}. All variables are binary with zero for not occurring or survival, and one for occurrence or failure.

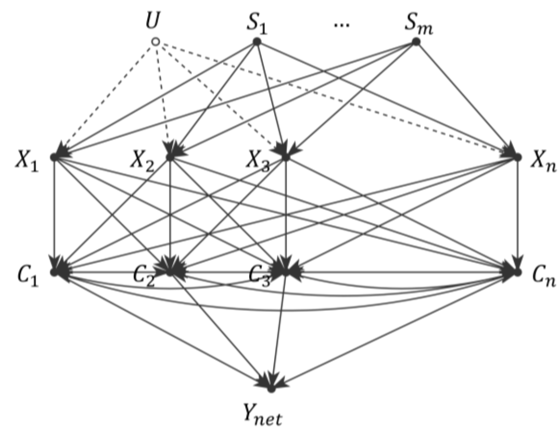

Figure 6: Causal diagram for network failure due to cascading component failures by multiple hazards.

From the proposed causal diagram, all the back doors from X_e and Y_{net} are blocked by the states of the remaining components, i.e., $X_{\hat{e}} = (X_1, X_2, \cdots, X_{e-1}, X_{e+1}, \cdots X_n)$. Then, the causal query, the probability with *do*-operator, can be computed with the conditional probabilities, i.e.,

$$P\big(Y_{net} = 1 \big| do(X_e = 1)\big)$$
$$= \sum_{X_{\hat{e}} \in \{0,1\}} P(Y_{net} = 1 | X_e = 1, X_{\hat{e}}) P(X_{\hat{e}}) \quad (14)$$

Since the S-DRA framework is performed scenario-wise, the contributions of individual components in the corresponding scenario are needed to propose a component-wise measure. $\mathcal{F}_{i,e}^{k}$ denotes the set with elements of all mutually exclusive and collectively exhaustive (MECE) events with the states of components in $I_i^k \backslash \{e\}$. Then the causal contribution component e in I_i^k to the system's performance is quantified as the change rate in the failure probability of the final system as X_e is switched from 0 to 1 along with the other components in $F \in \mathcal{F}_{i,e}^{k}$, i.e.,

$$r_e^k(F) = \begin{cases} 0 & P_e(F_{sys}|F) = 0 \\ 1 - \dfrac{P_{\bar{e}}(F_{sys}|F)}{P_e(F_{sys}|F)} & \text{otherwise} \end{cases} \quad (15)$$

where $P_e(F_{sys}|F) = P(Y_{net} = 1|do(X_e = 1), F)$, and $P_{\bar{e}}(F_{sys}|F) = P(Y_{net} = 1|do(X_e = 0), F)$.

Then, the merged contribution (MC) of component e to F_i^k is proposed as the summation of the products of the causal contribution in Eq. (15) and the occurrence probability for all elements in $\mathcal{F}_{i,e}^k$, i.e.,

$$MC_{i,e}^k = \sum\nolimits_{F \in \mathcal{F}_{i,e}^k} r_e^k(F) P(F|H) \quad (16)$$

A new causality-based decision-support measure is proposed by assigning the S-DRA results, the failure probabilities of the final system, from each scenario to the individual component belonging to the scenario. For the critical scenarios violating the resilience constraint, i.e., inducing a higher probability of the final system failure than the target resilience level, the causality-based decision-support measure (DM) and normalized DM (NDM) for component e are respectively proposed as

$$DM_e^k = \sum\nolimits_{i:R_i^k \notin \mathcal{D}_H} \Phi(-\pi_i^k)\Phi(-\beta_i^k) MC_{i,e}^k \quad (17)$$

$$NDM_e^k = \frac{DM_e^k}{\max_e(|DM_e^k|)} \quad (18)$$

The causality-based DM in Eq. (17) describes the weighted average of the contour values in the β-π diagram for the critical scenarios using MC in Eq. (16) as weights. NDM in Eq. (18) facilitates the comparison of components according to the initial disruptions of k components.

4.2. Application of the proposed measure to the power grid

Figure 7 shows the proposed NDM applied to the power grid for $\mathcal{D}_{\lambda_H}$ of the hazard with $\lambda_H = 1/2{,}500$ year. As k increases, the trend of NDM changes according to the causal relationship of the components that belong to the varying critical scenarios. For all k, the NDM of component *14* is 0, components *1* to *5* are positive, and the other components are negative consistently. The negative NDM comes from the cumulative negative values expressed with the *do*-operator in Eq. (15). It implies that the unconditional survival of a particular component does not always cause an improvement in the system reliability perspective.

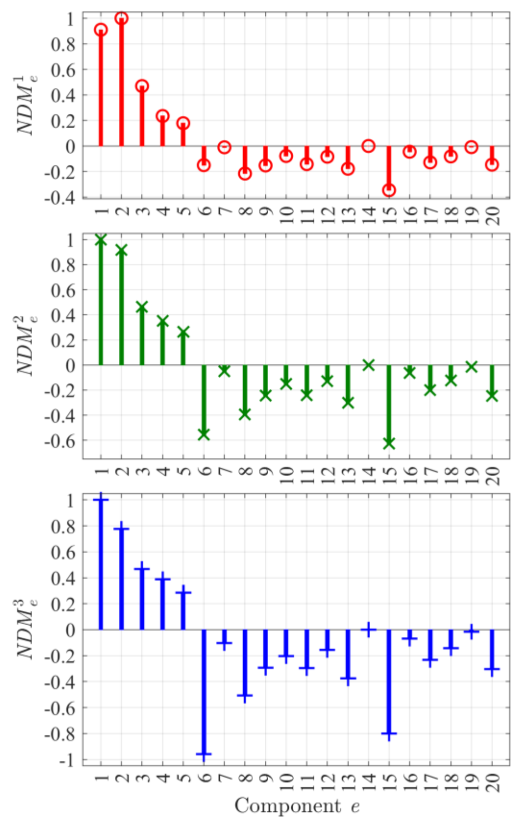

Figure 7: NDMs of the power grid for the mean occurrence rate $1/2{,}500\,year$.

Figure 8 shows the CIMs of the power grids. Since the definitions of RAW and RRW include the concept of *do*-operator, the signs and the trends with a reference point 1 are close to NDM^1. Compared to NDM, FV assigns zero importance to a significant number of components and shows opposite signs for some components. CP shows the trend of concentration on reliability rather than redundancy and fails to rule out spurious associations.

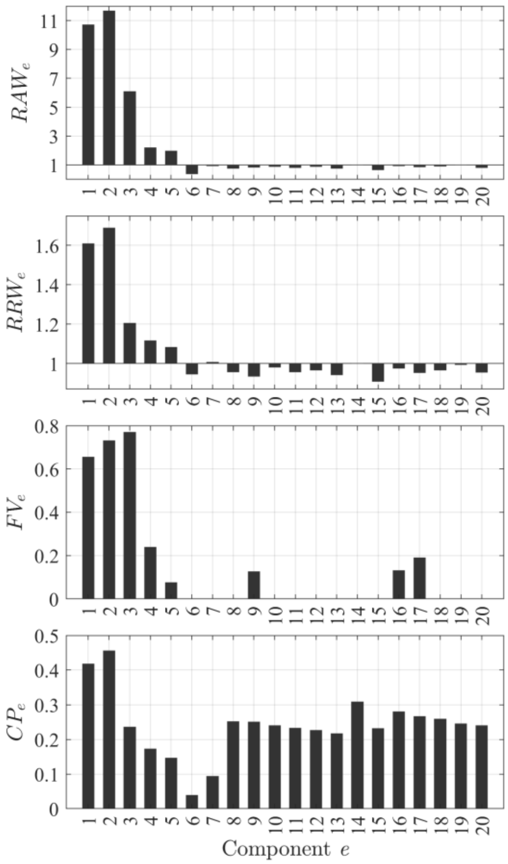

Figure 8: CIMs of the power grids: RAW, RRW, FV, and CP.

5. CONCLUSIONS

The system-reliability-based disaster resilience analysis (S-DRA) framework was applied to infrastructure networks, especially the power grid, considering the uncertainties of the response induced by a hazard. It was confirmed that the framework facilitates identifying the component criticality of the system-level performance by a comprehensive perspective combining reliability and redundancy. Based on the results of the β-π analysis we also proposed a new decision-support measure that can adaptively calculate the component importance according to the target resilience level, and balance the topological placement, electrical properties, and individual reliability. The measure is constructed component-wise based on the causality of the system-level performance degradation considering the operation mechanism of the power grid and the following cascading failure. An application of the proposed measure to the power grid verified its applicability to the general networks consisting of the components whose states are determined by the distributed flow in them. It is expected that the proposed measure will further enhance decision-making processes to secure the disaster resilience of infrastructure networks.

6. ACKNOWLEDGMENT

This research was supported by the National Research Foundation of Korea (NRF) Grant funded by the Korean government (NRF-2021R1A2C2003553).

7. REFERENCES

Boore, D.M., and Atkinson, G.M. (2008). “Ground-motion prediction equations for the average horizontal component of PGA, PGV, and 5%-damped PSA at spectral periods between 0.01s and 10.0s.” *Earthquake spectra*, 24(1), 99-138.

Bruneau, M., Chang, S.E., Eguchi, R.T., Lee, G.C., O’Rourke, T.D., Reinhorn, A.M., Shinozuka, M., Tierney, K., Wallace, W.A., and von Winterfeldt, D. (2003). “A framework to quantitatively assess and enhance the seismic resilience of communities.” *Earthquake spectra*, 19(4), 733-752.

Der Kiureghian, A. (2022). “Structural and system reliability.” *Cambridge University Press*.

Grainger, J.J. (1999). *Power system analysis*. McGraw-Hill.

Lee, D., and Song, J. (2021). “Multi-scale seismic reliability assessment of networks by centrality-based selective recursive decomposition algorithm.” *Earthquake Engineering & Structural Dynamics*, 50(8), 2174-2194.

Lim, S., Kim, T., and Song, J. (2022). “System-reliability-based disaster resilience analysis: Framework and applications to structural systems.” *Structural Safety*, 96, 102202.

Paté-Cornell, M. E. (1994). “Quantitative safety goals for risk management of industrial facilities.” *Structural Safety*, 13(3), 145-157.

Pearl, J. (2001). “Direct and indirect effects.” In *Proceedings of the Seventeenth Conference on Uncertainty in Artificial Intelligence (UAI'01). Morgan Kaufmann Publishers Inc., San Francisco, CA, USA*, 411-420.

Pearl, J. (2009). *Causality*. Cambridge university press.